Synthesis and Activity of 1,3,5-Triphenylimidazolidine-2,4-diones and 1,3,5-Triphenyl-2-thioxoimidazolidin-4-ones: Characterization of New CB_1 Cannabinoid Receptor Inverse Agonists/Antagonists

Giulio G. Muccioli,[†] Johan Wouters,[‡] Caroline Charlier,[‡] Gerhard K. E. Scriba,[§] Teresa Pizza,[†] Pierluigi Di Pace,[†] Paolo De Martino,[†] Wolfgang Poppitz,[||] Jacques H. Poupaert,[†] and Didier M. Lambert*[,†]

Unité de Chimie pharmaceutique et de Radiopharmacie, Ecole de Pharmacie, Faculté de Médecine, Université catholique de Louvain, Avenue E. Mounier 73, UCL-CMFA 7340, B-1200 Bruxelles, Belgium, Laboratoire de Chimie Biologique Structurale, Faculté des Sciences, University of Namur, Rue de Bruxelles 61, 5000 Namur, Belgium, Department of Pharmaceutical Chemistry, University of Jena, Philosophenweg 14, D-07743 Jena, Germany, and Department of Inorganic and Analytical Chemistry, University of Jena, August-Bebel-Strasse 2, D-07743 Jena, Germany

Received May 24, 2005

Obesity and metabolic syndrome, along with drug dependence (nicotine, alcohol, opiates), are two of the major therapeutic applications for CB_1 cannabinoid receptor antagonists and inverse agonists. In the present study, we report the synthesis and structure−affinity relationships of 1,5-diphenylimidazolidine-2,4-dione and 1,3,5-triphenylimidazolidine-2,4-dione derivatives. These new 1,3,5-triphenylimidazolidine-2,4-dione derivatives and their thio isosteres were obtained by an original pathway and exhibited interesting affinity and selectivity for the human CB_1 cannabinoid receptor. A [^{35}S]-GTPγS binding assay revealed the inverse agonist properties of the compounds at the CB_1 cannabinoid receptor. Furthermore, molecular modeling studies were conducted in order to delineate the binding mode of this series of derivatives into the CB_1 cannabinoid receptor. 1,3-Bis(4-bromophenyl)-5-phenylimidazolidine-2,4-dione (**25**) and 1,3-bis(4-chlorophenyl)-5-phenylimidazolidine-2,4-dione (**23**) are the imidazolidine-2,4-dione derivatives possessing the highest affinity for the human CB_1 cannabinoid receptor reported to date.

Introduction

The cloning of the cannabinoid CB_1 and CB_2 receptors in the early 1990s[1,2] followed by the discovery and characterization of their endogenous ligands—i.e. anandamide[3] (AEA) and 2-arachidonoylglycerol[4,5] (2-AG)—as well as the characterization of the enzymes responsible for endocannabinoid degradation—i.e. fatty acid amide hydrolase,[6] monoglyceride lipase,[7] and *N*-acylethanolamine-hydrolyzing acid amidase[8]—offered new areas for therapeutic interventions.[9] Clinical trials involving either cannabinoid receptor ligands or *Cannabis sativa* extracts[10] demonstrated pharmacological activities. For instance, Δ^9-tetrahydrocannabinol (Δ^9-THC) was recently shown to be effective in the treatment of Tourette's syndrome tics[11] and in the relief of pain.[12]

In this field, CB_1 cannabinoid receptor antagonists or inverse agonists exhibited interesting therapeutic potential while being devoid of psychotropic side effects.[13−15] The first reported CB_1 cannabinoid receptor inverse agonist, rimonabant[16] (SR141716A, Acomplia), was successfully tested in humans as treatment for obesity[17] (and associated metabolic syndrome) and smoking cessation (Figure 1).[18] Another promising application for such drugs is the treatment of drug dependence (alcohol, opiates, Δ^9-THC) as indicated by both animal and human studies.[19] Finally, recent studies in rats using the two inverse agonists SR141716A and LY320135 suggested that CB_1 cannabinoid receptor inverse agonists may be effective in reducing brain injury caused by focal ischemia.[20]

The wide application for CB_1 cannabinoid receptor antagonists or inverse agonists as pharmacological agents prompted the synthesis and characterization of new classes of compounds.[21] Indeed, in addition to the biarylpyrazoles (SR141716A, SR147778[22]), several other heterocyclic compounds such as triazoles,[23,24] thiazoles,[24] pyrazolines,[25] imidazoles,[24,26] and pyridines[27] have been described.

Along this line, our group previously reported the synthesis[28,29] and pharmacological characterization of 3-alkyl-5,5′-diphenylimidazolidine-2,4-dione[28,30] and 3-alkyl-5,5′-diphenyl-2-thioxoimidazolidin-4-one[31] derivatives as cannabinoid ligands. These compounds, exhibiting moderate affinity, act as selective inverse agonists at the CB_1 cannabinoid receptor. The structure−affinity relationships obtained to date revealed three important features to enhance the affinity toward the receptor: (i) the N_3 nitrogen must be substituted, (ii) introduction of an halogen substituent in para position of the phenyl rings increases the affinity, (iii) thio derivatives are more active than the corresponding oxo derivatives.

In the present study, new substitution patterns of the imidazolidine-2,4-dione ring, leading to the 1,5-diphenylimidazolidine-2,4-dione and to the 1,3,5-triphenylimidazolidine-2,4-dione series, were explored as new potential human CB_1 cannabinoid receptor ligands. The latter series of compounds was synthesized in good yields by a previously unreported method from phenylglyoxal and 1,3-diphenylurea. The pharmacological properties of 1,5-diphenylimidazolidine-2,4-dione (**6**−**18**), 1,3,5-triphenylimidazolidine-2,4-dione (**20**−**29**), and 1,3,5-triphenyl-2-thioxoimidazolidin-4-one (**30**−**38**) derivatives at the human CB_1 cannabinoid receptor were characterized. Finally, the results allowed the establishment of structure−activity relationships, aiming at the characterization of this new series of CB_1 cannabinoid receptor inverse agonists.

* Corresponding author. Phone: +32 2 7647347. Fax: +32 2 7647363. lambert@cmfa.ucl.ac.be.
[†] Université catholique de Louvain.
[‡] University of Namur.
[§] Department of Pharmaceutical Chemistry, University of Jena.
[||] Department of Inorganic and Analytical Chemistry, University of Jena.

10.1021/jm050484f CCC: $33.50
Published on Web 01/13/2006

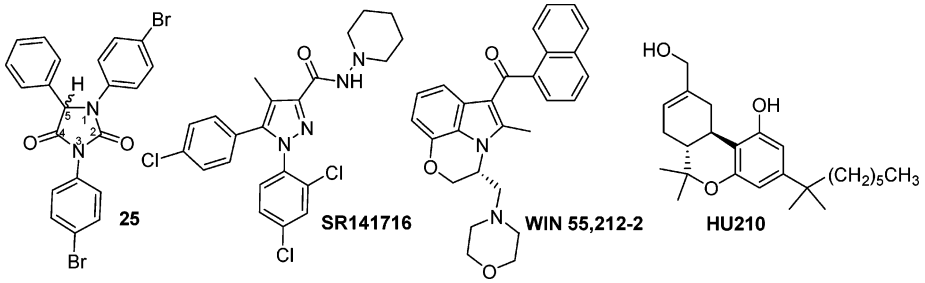

Figure 1. Structures of derivative **25** and of SR141716, WIN-55,212-2, and HU-210.

Scheme 1. Synthesis of the 1,5-Diphenylimidazolidine-2,4-dione (**6**, **8**−**18**) and 1,5-Diphenyl-2-thioxoimidazolidin-4-one (**7**) Derivatives[a]

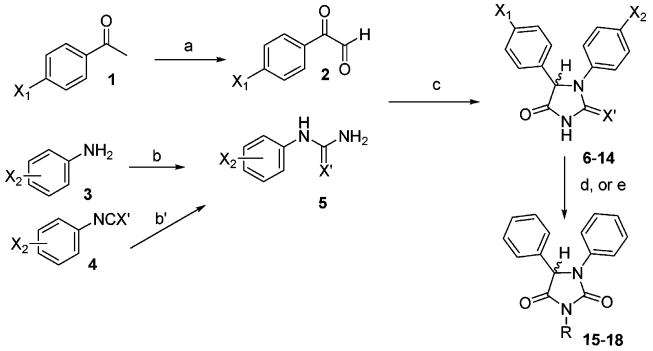

[a] Reagents and conditions: (a) SeO_2, dioxane−water (70:4), 55 °C, overnight; (b) CH_3COOH/H_2O, NaOCN, rt; (b′) acetone, NH_4OH, rt; (c) CH_3COOH−HCl (15:0.5), reflux, 4 h; (d) CH_2Cl_2, pyridine, COCl−R, rt, overnight; (e) DMF, K_2CO_3, tetrabutylammonium bromide, Cl−R, 3 × 1.5 min microwave pulses (100 W).

Results and Discussion

Chemistry. Substituted phenylglyoxal derivatives (**2**, X_1 = Cl, Br) were synthesized from the corresponding acetophenones (**1**) using selenium dioxide as oxidant according to a method described by Riley and Gray[32] (Scheme 1). Distillation of the resulting oil (substituted phenylglyoxal) followed by recrystallization from water was usually sufficient to remove selenium contaminants from substituted phenylglyoxal.

Substituted phenylurea derivatives (**5**, X′ = O) were easily obtained in high yields by reacting the corresponding aniline (**3**) with sodium cyanate in an acetic acid−water mixture[33] (Scheme 1). The reaction was almost complete, and the resulting phenylureas were used without further purification. The phenylthiourea (**5**, X′ = S) was obtained in high yields by reacting phenyl isothiocyanate (**4**, X′ = S) with ammonia.

The 1,5-diphenylimidazolidine-2,4-dione derivatives (**6**, **8**−**14**, X′ = O) were synthesized from phenylglyoxal and phenylurea by slightly modifying the procedure described by Joshi et al.[34] (Scheme 1). Four hours of reflux in an acetic acid−hydrochloric acid mixture yielded the 1,5-diphenylimidazolidine-2,4-dione derivatives in good yields (59−64%). The same procedure using phenythiourea afforded the 1,5-diphenyl-2-thioxoimidazolidin-4-one (**7**, X′ = S).

Derivatives **15** and **16** were obtained in high yields by acylation of **6** with benzoyl chloride and hexanoyl chloride, respectively, in a CH_2Cl_2−pyridine mixture (Scheme 1). Derivatives **17** and **18** were prepared by alkylation of **6** using a microwave-assisted procedure adapted from Bogdal et al.[35] (Scheme 1).

Reacting the aniline **3** with phenyl isocyanate (**4**, X′ = O) and phenyl isothiocyanate (**4**, X′ = S) afforded in good yields the 1,3-diphenylurea (**19**, X′ = O) and 1,3-diphenylthiourea (**19**, X′ = S) derivatives, respectively (Scheme 2).

Scheme 2. Synthesis of the 1,3,5-Triphenylimidazolidine-2,4-dione (**20**−**29**) and 1,3,5-Triphenyl-2-thioxoimidazolidin-4-one (**30**−**38**) Derivatives[a]

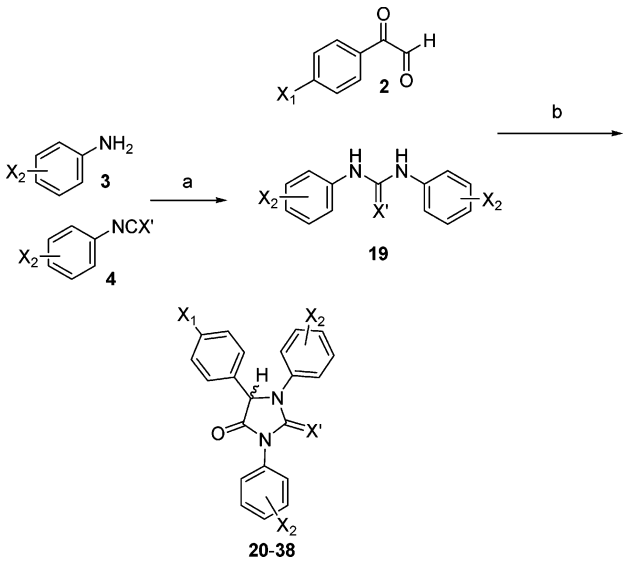

[a] Reagents and conditions: (a) acetone, rt, 6 h; (b) CH_3COOH−HCl (20:0.5), reflux, 6 h.

The target 1,3,5-triphenylimidazolidine-2,4-dione derivatives (**20**−**29**) were obtained by an original pathway starting from 1,3-diphenylurea (**19**, X′ = O) and phenylglyoxal (**2**) as described in Scheme 2. This reaction represents a simple one-pot procedure to obtain in moderate to good yields **20**−**29**. However, it has to be mentioned that this reaction pathway does not allow for the synthesis of enantiopure compounds. The structure of the triphenylimidazolidine-2,4-dione products was confirmed by the X-ray diffraction of compound **22** (Figure 2). Interestingly, spontaneous resolution was observed upon crystallization. Indeed, the crystallization conditions of **22** yielded crystals presenting a preferential enrichment of the *R* enantiomer (3:1 ratio for the *R*/*S* enantiomers) starting from a racemic mixture of the product. Similar spontaneous resolution of racemic mixtures, although rarely observed in the natural work, has been reported in other series of molecules, in particular for 1,3,5-triphenyl-2-pyrazoline.[36]

No classical H-bond is observed within the crystal packing of **22**. This is explained by the lack of any suitable H-bond donor within the molecule. In particular, substitution of N_1 by a phenyl eliminates this center as sole potential H-bond donor, in contrast with what is observed with N_1 unsubstituted analogues.[29,31] Interestingly, short intramolecular C−H···O bonds (2.6−3.0 Å) involve the oxygen atoms in position O_1 and the H atoms in the ortho positions of the aromatic rings substituting both N atoms. These intramolecular interactions influence the conformation and relative orientation of the aromatics around

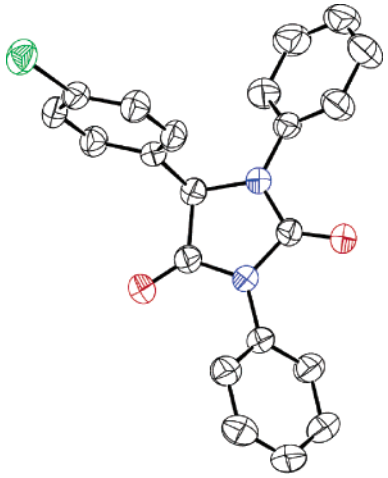

Figure 2. ORTEP diagram of **22** representing one molecule of the asymmetric unit. Both enantiomers were present in the crystal.

the imidazolidine-2,4-dione scaffold and could play a role during the binding to the receptor.

Crystal cohesion of **22** mainly results from stacking interactions that involve the π-system of the aromatic rings. All three phenyl rings are involved in these intermolecular interactions. In addition, the central imidazolidine-2,4-dione ring is engaged in T-shape perpendicular interactions with neighboring molecules. The CO bond of one imidazolidine-2,4-dione ring points to the center of an imidazolidine-2,4-dione ring of a symmetry-related molecule.

Taken together, the crystallographic data obtained on **22** confirm the structure of the compound and the presence of both enantiomers in the mixture. They further suggest that the central imidazolidine-2,4-dione ring could influence the relative orientation of the aromatic substituents within the molecule (through intramolecular H-bonds), allowing them to form proper π-stacking interactions with residues of the protein during binding to a receptor. The conformation of **22** obtained by X-ray crystallography is also an excellent starting point for modeling of the different 1,3,5-triphenylimidazolidine-2,4-dione derivatives (**20**−**29**) within the CB_1 cannabinoid receptor, as discussed further in the text.

Using 1,3-diphenylthiourea (**19**, X′ = S) instead of the urea derivative, the 1,3,5-triphenyl-2-thioxoimidazolidin-4-one derivatives were similarly obtained (**30**−**38**, Scheme 2). Except for the iodo derivative (**35**), yields were not influenced by the phenyl substituents (X_1 and X_2). 1,3-Bis(4-hydroxyphenyl)-5-phenyl-2-thioxoimidazolidin-4-one (**38**) was obtained in high yield from the methoxy derivative (**37**) by demethylation using boron tribromide.

1,3-Dicyclohexyl-5-phenylimidazolidine-2,4-dione (**40**) was synthesized from 1,3-dicyclohexylurea (**39**) and phenylglyoxal (**2**) as illustrated in Scheme 3.

Pharmacology−**Affinity toward the Cannabinoid Receptors.** All the compounds were screened at 10 μM concentrations for competitive binding to the human cannabinoid receptors CB_1 and CB_2 in a competitive binding experiment, using membranes of Chinese hamster ovarian (CHO) cells selectively expressing either the human CB_1 (hCB_1) or CB_2 (hCB_2) cannabinoid receptor. [^{3}H]-SR141716A and [^{3}H]-CP-55,940 were used as radioligands (1 nM) in these experiments for the hCB_1 and hCB_2 cannabinoid receptor, respectively. Table 1 summarizes the results expressed as the displacement percentages of the radioligand from its binding site for the 1,5-diphenylimidazolidine-2,4-dione and 1,5-diphenyl-2-thioxoimidazolidin-4-one

Scheme 3. Synthesis of 1,3-Dicyclohexyl-5-phenylimidazolidine-2,4-dione (**40**)[a]

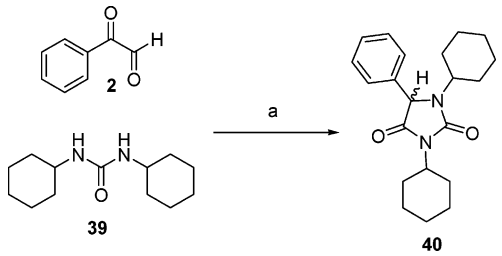

[a] Reagents and conditions: (a) CH_3COOH−HCl (20:0.5), reflux, 10 h.

Table 1. Percentages of Displacement of [^{3}H]-SR141716A and [^{3}H]-CP-55,940, Respectively, by Synthesized 1,5-Diphenylimidazolidine-2,4-diones (10 μM) on hCB_1 and hCB_2 Cannabinoid Receptors[a]

					% displacement	
compd	X′	X_1	X_2	R	hCB_1 receptor	hCB_2 receptor
6	O	H	H	H	<10	<10
7	S	H	H	H	<10	<10
8	O	H	Cl	H	<15	<10
9	O	H	Br	H	25.2 ± 1.2	<10
10	O	H	I	H	<20	<10
11	O	H	OMe	H	<10	<10
12	O	Br	H	H	<15	<10
13	O	Br	Cl	H	<15	<10
14	O	Br	Br	H	<15	<10
15	O	H	H	CO-C_6H_5	<10	<10
16	O	H	H	CO-C_5H_{11}	<10	<10
17	O	H	H	C_5H_{11}	41.1 ± 1.2	<10
18	O	H	H	C_7H_{15}	45.6 ± 3.5	<10

[a] Mean ± SEM of at least four experiments performed in duplicate.

derivatives (**6**−**14**). None of the compounds (**6**−**14**), assayed as racemic mixtures, displayed significant competitive binding toward either the hCB_1 or hCB_2 cannabinoid receptor. Therefore, on the basis of the structure−affinity relationships obtained with the 5,5′-diphenylimidazolidine-2,4-dione and 5,5′-diphenyl-2-thioxoimidazolidin-4-one derivatives which showed the importance of the substitution of the nitrogen in position 3,[28,30−31] four N_3-substituted compounds were synthesized and assayed for their affinity (**15**−**18**). The acylated derivatives **15** (N_3-benzoyl) and **16** (N_3-hexanoyl) were both devoid of affinity for the cannabinoid receptors. However, as expected, the introduction of an alkyl moiety (**17** and **18**) resulted in an increased affinity for the hCB_1 cannabinoid receptor with displacement percentages around 40%.

In a second group of compounds, derivatives possessing an additional phenyl ring in position 3 were synthesized, leading to the 1,3,5-triphenylimidazolidine-2,4-dione series of derivatives (**20**−**29**, X′ = O). Screening results for this series of compounds are summarized in Table 2. The hCB_1 cannabinoid receptor affinity was greatly enhanced by the presence of an additional phenyl ring, as the radioactivity displacement is above 50% for all the compounds. This is further illustrated by compounds **6** and **20** (<10% and 57% displacement at 10 μM, respectively) and by compounds **12** and **22** (<15% and 75% displacement at 10 μM, respectively). It has to be mentioned that the hCB_2 cannabinoid receptor affinity was also improved, although to a much lower extent than the hCB_1 cannabinoid receptor affinity.

The 1,3,5-triphenyl-2-thioxoimidazolidin-4-one derivatives (**30**−**38**), which are the thio isosteres of the 1,3,5-triphenylimidazolidine-2,4-diones, were also obtained and assayed for their affinity at the cannabinoid receptors (Table 2). In this series,

Table 2. Percentages of Displacement of [^{3}H]-SR141716A and [^{3}H]-CP-55,940, Respectively, by 1,3,5-Triphenylimidazolidine-2,4-diones and 1,3,5-Triphenyl-2-thioxoimidazolidin-4-ones (10 μM) on hCB$_1$ and hCB$_2$ Cannabinoid Receptors[a] and Percentages of FAAH Activity (rat brain homogenate) Inhibition by 1,3,5-Triphenylimidazolidine-2,4-diones and 1,3,5-Triphenyl-2-thioxoimidazolidin-4-ones (10 μM)[a]

				% displacement		
compd	X′	X_1	X_2	hCB$_1$ receptor	hCB$_2$ receptor	% FAAH inhibition
			Imidazolidine-2,4-dione Derivatives			
20	O	H	H	57.1 ± 1.5	<10	<10
21	O	Cl	H	60.2 ± 1.8	<15	13.7 ± 3.5
22	O	Br	H	75.4 ± 2.1	<15	14.5 ± 4.4
23	O	H	4-Cl	101.1 ± 1.5	21.6 ± 2.3	<10
24	O	H	3-Cl	76.0 ± 2.2	32.1 ± 1.6	<10
25	O	H	4-Br	102.1 ± 1.9	35.6 ± 1.9	<10
26	O	H	4-OMe	57.8 ± 3.1	31.4 ± 2.1	<10
27	O	Cl	4-Cl	71.6 ± 2.1	28.1 ± 2.3	<10
28	O	Cl	3-Cl	67.4 ± 2.4	24.8 ± 3.1	<10
29	O	Br	4-Cl	79.1 ± 3.1	<20	15.4 ± 2.5
			2-Thioxoimidazolidin-4-one Derivatives			
30	S	H	H	61.7 ± 1.7	<10	11.8 ± 3.6
31	S	Br	H	85.1 ± 3.7	<10	19.1 ± 2.5
32	S	H	4-Cl	93.7 ± 3.1	<10	11.4 ± 2.4
33	S	H	3,4-diCl	78.7 ± 1.5	<10	22.9 ± 1.7
34	S	H	4-Br	100.1 ± 1.3	<15	<10
35	S	H	3-I	81.2 ± 1.8	<15	17.4 ± 2.4
36	S	H	4-Me	80.1 ± 2.1	<20	<10
37	S	H	4-OMe	65.6 ± 3.1	<20	<10
38	S	H	4-OH	<20	<10	31.5 ± 2.3

[a] Mean ± SEM of at least four experiments performed in duplicate.

the affinity was also enhanced by the phenyl in position 3, as demonstrated by compounds **7** and **30** (<10% and 62% displacement at 10 μM, respectively). Meanwhile, the hCB$_2$ cannabinoid receptor affinity was not affected by this modification.

To estimate the influence of the aromatic ring in positions 1 and 3, 1,3-dicyclohexyl-5-phenylimidazolidine-2,4-dione (**40**) was tested (at 10 μM) in a binding assay. This compound displaced around 25% of the [^{3}H]-SR141716, compared to the 57% displacement obtained with **20**, confirming the important role of the phenyl rings in positions 1 and 3.

To study the structure−affinity relationships, the inhibition constants (K_i) of the derivatives showing the highest radioligand displacement (>55%) were determined. The K_i values are summarized in Table 3. With respect to the imidazolidine-2,4-dione series, a bromine or a chlorine substituent in the para position of the N_1 and N_3 phenyl rings (X_2, Scheme 2 and Table 3) strongly enhances the affinity, as illustrated by derivatives **20** (X_2 = H), **23** (X_2 = Cl), and **25** (X_2 = Br), exhibiting K_i values of 6296 ± 354 nM, 353 ± 34 nM, and 243 ± 18 nM, respectively. A methoxy substituent in the same position (**26**, X_2 = OMe) has no effect on the affinity (K_i = 6456 ± 354 nM). Further, it appears that substitution at the para position is preferred to the meta position, as revealed by compounds **23** and **24** bearing a chlorine substituent (X_2) in the para and meta positions, respectively (K_i values of 353 ± 34 nM and 2110 ± 99 nM for **23** and **24**, respectively). Moreover, chlorine and bromine substituents in the para position of the C_5 phenyl ring (X_1) are responsible for a decreased affinity. For example, derivatives **27** (X_1 = Cl) and **29** (X_1 = Br) exhibited lower K_i values than derivative **23** (X_1 = H). The highest affinities were obtained for 1,3-bis(4-chlorophenyl)-5-phenylimidazolidine-2,4-dione (**23**) and 1,3-bis(4-bromophenyl)-5-phenylimidazolidine-2,4-dione (**25**) with K_i values of 353 ± 34 and 243 ± 18 nM, respectively.

In the 2-thioxoimidazolidin-4-one series, the X_2 substituent effect is conserved as illustrated by compounds **30** (X_2 = H), **32** (X_2 = Cl), and **34** (X_2 = Br), showing K_i values of >8000, 2163 ± 84, and 1447 ± 54 nM, respectively. A methyl substituent (**36**, X_2 = Me) induces a slight affinity increase but to a lower extent compared to a halogen substituent. The highest affinity in this series was obtained with 1,3-bis(3-iodophenyl)-5-phenyl-2-thioxoimidazolidin-4-one (**35**), exhibiting a K_i value of 692 ± 34 nM.

Table 3. Affinities of **20**−**37** and Reference Cannabinoids SR141716A, WIN-55,212-2, and HU-210 at the hCB$_1$ Cannabinoid Receptor[a] and Determination of the Potency (EC_{50}) and Maximal Stimulation (E_{max}) for Compounds **23**−**25**, **27**, **29**, **32**, **34**, **35** and for HU-210 and SR141716A on hCB$_1$ Cannabinoid Receptors[b]

					activity	
compd	X′	X_1	X_2	affinity K_i (nM)	EC_{50} (nM)	E_{max} (%)
			Imidazolidine-2,4-dione Derivatives			
20	O	H	H	6296 ± 354	/	/
21	O	Cl	H	6661 ± 386	/	/
22	O	Br	H	4027 ± 276	/	/
23	O	H	4-Cl	353 ± 34	309 ± 31	−74.4 ± 1.3
24	O	H	3-Cl	2110 ± 99	936 ± 74	−50.9 ± 1.4
25	O	H	4-Br	243 ± 18	195 ± 24	−75.1 ± 1.2
26	O	H	4-OMe	6456 ± 354	/	/
27	O	Cl	4-Cl	1877 ± 87	1115 ± 86	−45.2 ± 1.6
28	O	Cl	3-Cl	3312 ± 167	/	/
29	O	Br	4-Cl	905 ± 42	1234 ± 64	−48.6 ± 1.7
			2-Thioxoimidazolidin-4-one Derivatives			
30	S	H	H	>8000	/	/
31	S	Br	H	6309 ± 304	/	/
32	S	H	4-Cl	2163 ± 84	2103 ± 174	−51.9 ± 2.5
33	S	H	3,4-diCl	2001 ± 73	/	/
34	S	H	4-Br	1447 ± 54	1624 ± 123	−35.7 ± 1.7
35	S	H	3-I	692 ± 34	461 ± 43	−19.3 ± 0.8
36	S	H	4-Me	4968 ± 264	/	/
37	S	H	4-OMe	7033 ± 321	/	/
			Reference Cannabinoids			
SR141716A				5.4 ± 0.2	10.1 ± 0.7	−84.1 ± 1.7
WIN-55,212-2				3802 ± 158	/	/
HU-210				18.6 ± 1.7	0.6 ± 0.04	201.2 ± 14.1

[a] K_i values were obtained from nonlinear analysis of competition curves using [^{3}H]-SR141716A as radioligand. Mean ± SEM of at least four experiments done in duplicate. [b] Mean ± SEM of at least four experiments performed in duplicate.

The structure−affinity relationships among the 3-alkyl-5,5′-diphenyl derivatives have demonstrated an affinity increase induced by replacement of the carbonyl by a thiocarbonyl in position 2 of the imidazolidine-2,4,dione ring.[31] In the 1,3,5-triphenyl derivatives series (**20**−**38**) the opposite situation occurred. For instance, the oxo derivative 1,3-bis(4-chlorophenyl)-5-phenylimidazolidine-2,4-dione (**23**) showed a higher affinity than its thio homologue 1,3-bis(4-chlorophenyl)-5-phenyl-2-thioxoimidazolidin-4-one (**32**) (K_i values of 353 ± 34 and 2163 ± 84 nM, respectively), and 1,3-bis(4-bromophenyl)-5-phenylimidazolidine-2,4-dione (**25**) exhibited a lower K_i value than 1,3-bis(4-bromophenyl)-5-phenyl-2-thioxoimidazolidin-4-one (**34**) (K_i values of 243 ± 18 and 1447 ± 54 nM, respectively).

Pharmacology. CB_1 Cannabinoid Receptor Recognition and Fatty Acid Amide Hydrolase Inhibition. The demonstration of fatty acid amide hydrolase (FAAH) inhibition by several 2-thioxoimidazolidin-4-one and imidazolidine-2,4-dione derivatives[37] prompted us to determine the potential of 1,3,5-triphenylimidazolidine-2,4-dione and 1,3,5-triphenyl-2-thioxoimidazolidin-4-one derivatives for inhibition of FAAH. Compounds **20**−**38** were screened at 10 μM concentrations for their ability to inhibit tritiated anandamide degradation in the presence of rat brain homogenates. The results are summarized in Table 2. Imidazolidine-2,4-dione derivatives were not able

to inhibit FAAH activity, as inhibition percentages were lower than 15%. Thus, the presence of three phenyl rings around the imidazolidine-2,4-dione moiety enhances CB_1 cannabinoid receptor affinity, without affecting FAAH activity. 2-Thioxoimidazolidin-4-one derivatives also exhibited poor activity as FAAH inhibitors, further confirming the selectivity achieved with the 1,3,5-triphenyl substitution pattern for the CB_1 cannabinoid receptor.

Functionality at the CB_1 Cannabinoid Receptors. 3-Alkyl-5,5′-diphenylimidazolidine-2,4-dione and 3-alkyl-5,5′-diphenyl-2-thioxoimidazolidin-4-one derivatives were previously shown to behave as inverse agonists at the *h*CB_1 cannabinoid receptor. Therefore, the functionality of 1,3,5-triphenylimidazolidine-2,4-dione (**20**−**29**) and 1,3,5-triphenyl-2-thioxoimidazolidin-4-one (**31**−**36**) derivatives was explored using a [^{35}S]-GTPγS assay.[38] GDP−GTP exchange is an early event in the signal transduction mechanism of a G-protein-coupled receptor (GPCR). Thus, measuring the [^{35}S]-GTPγS—a radiolabeled nonhydrolyzable analogue of GTP—binding provides a direct measurement of the interaction between the receptor and the G protein upon binding of an agonist to the GPCR. Actually, agonist binding to a receptor will increase the guanine nucleotide binding, a neutral antagonist will not influence the nucleotide binding, and finally, an inverse agonist will decrease the [^{35}S]-GTPγS binding to the G protein.

Derivatives possessing a K_i value at the *h*CB_1 cannabinoid receptor lower than 7000 nM were screened at a 10 μM concentration, along with HU-210 and SR141716A, a known agonist and an inverse agonist, respectively. As expected, 10 μM SR141716A and HU-210 induced a decrease (−79% compared to basal) and an increase (129% compared to basal level), respectively, in the [^{35}S]-GTPγS binding (Figure 3). The 1,3,5-triphenylimidazolidine-2,4-dione (**20**−**29**) and 1,3,5-triphenyl-2-thioxoimidazolidin-4-one (**31**, **32**, **34**−**36**) derivatives induced a significant decrease in [^{35}S]-GTPγS binding, ranging from −12% to −70%, with the notable exception of derivative **33**, which did not induced any significant variation in nucleotide binding (Figure 3). The observed decrease in [^{35}S]-GTPγS binding revealed the inverse agonist properties of the series of imidazolidine-2,4-dione and 2-thioxoimidazolidin-4-one derivatives at the *h*CB_1 cannabinoid receptor. Thus with respect to the imidazolidine-2,4-dione and 2-thioxoimidazolidin-4-one substitution pattern, the 1,3,5-triphenyl derivatives behaved as the 3-alkyl-5,5′-diphenyl derivatives at the *h*CB_1 cannabinoid receptor. The activity of compounds **32** and **33** deserves some attention. Indeed, while both compounds exhibited similar affinity ($K_i \sim 2100$ nM), the [^{35}S]-GTPγS assay evidenced different activities, i.e. inverse agonism for **32** and antagonism for **33**. The additional chlorine substituent in the meta position induced an activity change, revealing a modified binding position to the receptor. This finding should be helpful in further studies aimed at understanding the molecular parameters inducing the inverse agonism and/or antagonism of this series of compounds.

To further explore the inverse agonist properties, potencies of imidazolidine-2,4-diones **23**-**25**, **27**, and **29** and 2-thioxoimidazolidin-4-ones **32**, **34**, and **35** were determined by measuring the decrease in nucleotide binding induced by increasing concentrations of test compounds. The respective EC_{50} and E_{max} values are summarized in Table 3. The compounds possessing the highest affinity, 1,3-bis(4-chlorophenyl)-5-phenylimidazolidine-2,4-dione (**23**), 1,3-bis(4-bromophenyl)-5-phenylimidazolidine-2,4-dione (**25**), and 1,3-bis(3-iodophenyl)-5-phenyl-2-thioxoimidazolidin-4-one (**35**), exhibited also the highest potency

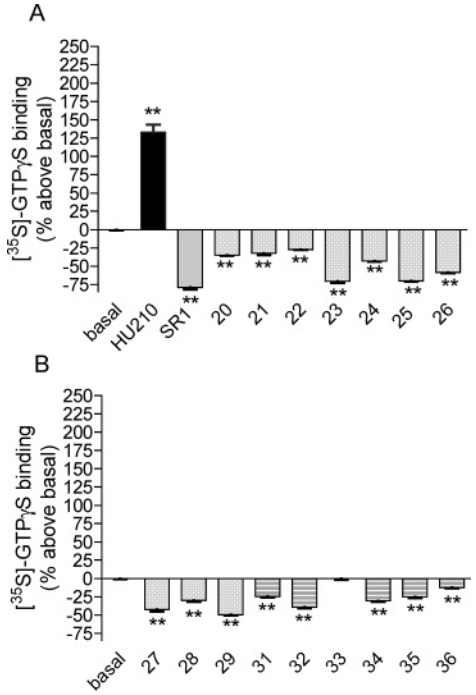

Figure 3. (A) [^{35}S]-GTPγS binding stimulation assay of 1,3,5-triphenylimidazolidine-2,4-dione (**20**−**26**) derivatives, and of SR141716A (SR1) and HU-210 (10 μM) on the *h*CB_1 cannabinoid receptor. Data are expressed as the mean ± SEM of at least three experiments performed in duplicate. Statistical significance assessed by one-way ANOVA followed by a Dunett post-test (**$P < 0.01$). (B) [^{35}S]-GTPγS binding stimulation assay of 1,3,5-triphenylimidazolidine-2,4-dione (**27**−**29**) derivatives and of 1,3,5-triphenyl-2-thioxoimidazolidin-4-one (**31**−**36**) derivatives (10 μM) on the *h*CB_1 cannabinoid receptor. Data are expressed as the mean ± SEM of at least three experiments performed in duplicate. Statistical significance assessed by one-way ANOVA followed by a Dunett post-test (**$P < 0.01$).

at the *h*CB_1 cannabinoid receptor with EC_{50} values of 309 ± 31, 195 ± 24, and 461 ± 43 nM, respectively.

As observed in the affinity studies, the thio derivatives exhibited lower potency and efficacy compared to the imidazolidine-2,4-dione derivatives. This is well-demonstrated by compounds **23** and **32** (EC_{50} values of 309 ± 31 and 2103 ± 174 nM, respectively; E_{max} values of −74.4 ± 1.3 and −51.9 ± 2.5%, respectively) or by compounds **25** and **34** (EC_{50} values of 195 ± 24 nM and 1624 ± 123 nM, respectively; E_{max} values of −75.1 ± 1.2 and −35.7 ± 1.7%, respectively).

3-Alkyl-5,5′-bis(4-bromophenyl)imidazolidine-2,4-dione derivatives reported to act as inverse agonists at the human CB_1 cannabinoid receptor expressed in CHO cells (*h*CB_1-CHO) were also shown to behave as neutral antagonists at the rat CB_1 cannabinoid receptor expressed in cerebellum homogenates (*r*CB_1).[39,28] Thus, to determine if this behavior is shared by the 1,3,5-triphenylimidazolidine-2,4-diones, the affinity and functionality of derivatives **23**, **25**, **27**, and **29** at the murine CB_1 receptor were determined. On one hand, K_i values at the *r*CB_1 cannabinoid receptor (Table 4) are of the same magnitude compared to those obtained at the *h*CB_1 cannabinoid receptor (Table 3). On the other hand, derivatives **23**, **25**, **27**, and **29** at 10 μM concentrations did not influence the [^{35}S]-GTPγS binding, thus revealing neutral antagonistic properties at the *r*CB_1 cannabinoid receptor (Figure 4). In general, 1,3,5-triphenylimidazolidine-2,4-dione derivatives exhibited the same behavior as 3-alkyl-5,5′-bis(4-bromophenyl)-imidazolidine-2,4-diones at the human and murine CB_1 cannabinoid receptors.

Table 4. Determination of the Affinities of **23**, **25**, **27**, and **29** at the *r*CB_1 Cannabinoid Receptor, Compared to Those of Reference Cannabinoids SR141716A and HU-210[6]

compd	*r*CB_1 (cerebellum) K_i (nM)	compd	*r*CB_1 (cerebellum) K_i (nM)
23	247 ± 25	**29**	1744 ± 91
25	311 ± 21	SR141716A	1.23 ± 0.1
27	2618 ± 104	HU-210	2.75 ± 0.2

[a] K_i values were obtained from nonlinear analysis of competition curves using [^{3}H]-SR141716A as radioligand. Mean ± SEM of at least four experiments done in duplicate.

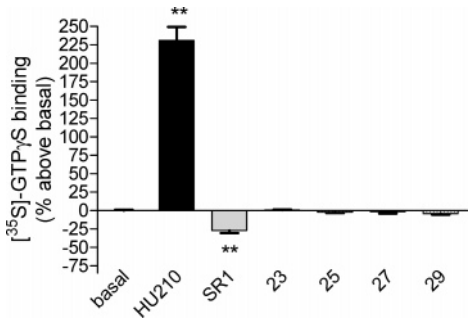

Figure 4. [^{35}S]-GTPγS binding stimulation assay of 1,3,5-triphenylimidazolidine-2,4-dione (**23**, **25**, **27**, **29**) derivatives and of SR141716A (SR1) and HU-210 (10 μM) on the *r*CB_1 cannabinoid receptor (rat cerebellum homogenate). Data are expressed as the mean ± SEM of at least three experiments performed in duplicate. Statistical significance assessed by one-way ANOVA followed by a Dunett post-test (**P < 0.01)

Molecular Modeling. To assess the influence of stereochemistry on the *h*CB_1 cannabinoid receptor affinity, the binding modes of both enantiomers of **25**, the most active compound in the imidazolidine-2,4-dione series, have been explored and compared with that of the reference inverse agonist SR141716A. The binding of the latter has recently been modeled inside the *h*CB_1 receptor[40] and correlates well with the established mutagenesis studies.[41] It involves direct aromatic stacking interactions with F3.36, Y5.39, W5.43, and W6.48, as well as a hydrogen bond with K3.28.

We manually docked SR141716A into the inactive R-state of the CB_1 receptor model in order to reproduce the interaction pattern described in the literature. Then, the *R*- and *S*-enantiomers of **25**, which act as inverse agonists too, were docked into the inactive R-state of the cannabinoid receptor. As we had no a priori knowledge on their mode of interaction, we explored their binding with the help of the automated GOLD docking software.[42] All the receptor−ligand complexes were finally refined by molecular mechanics,[43] allowing the active site's side chains to accommodate the ligand.

As illustrated in Figures 5 and 6, both enantiomers of **25** adopt a similar orientation within the CB_1 cannabinoid receptor. The interaction pattern of **25** seems to be governed by the binding of the two bromophenyls to the aromatic microdomain. Indeed, these two rings form several direct stacking interactions with the aromatic microdomain and especially with F3.36, Y5.39, and W5.43. Furthermore, in both cases, the unsubstituted phenyl interacts strongly through an aromatic contact with F6.32. Orientation of the two N-substituent phenyl rings is stabilized by intramolecular C−H···O bonds involving a carbonyl oxygen of the imidazolidine-2,4-dione moiety. Similar interactions were suggested on the basis of the crystal structure of **22** and are probably a characteristic of this series of molecules.

However, this orientation involves, for the *R*-enantiomer, inversion of the central imidazolidine-2,4-dione ring in comparison with the *S*-enantiomer and prevents the formation of a hydrogen bond with K3.28. In contrast, the *S*-enantiomer realizes a hydrogen bond with K3.28 similarly to SR141716A, which also interacts through hydrogen bonding with this residue. This particular interaction has been shown to account for the higher affinity of SR141716A for the inactive R-state, leading to its inverse agonism.[41] This binding difference between *R*- and *S*-enantiomers suggests a strong influence of stereochemistry on CB_1 cannabinoid receptor affinity for **25**.

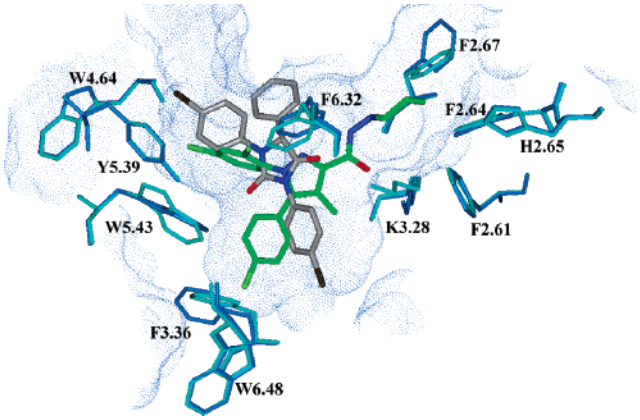

Figure 5. Superimposition of the complex of SR141716A and the CB_1 cannabinoid receptor model (colored in green and blue, respectively) with the complex of ***S*-25** and the CB_1 cannabinoid receptor model (colored in gray and cyan, respectively). The representation of the Connolly surface (probe 1.4 Å) defines the accessible binding pocket.

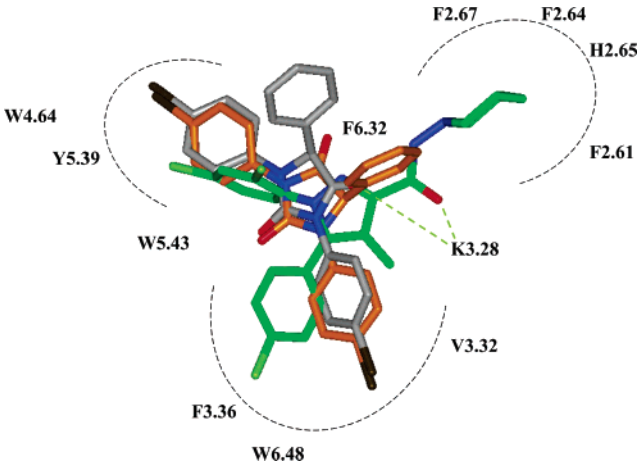

Figure 6. Receptor-based alignment of SR141716A (in green), ***S*-25** (in gray), and ***R*-25** (in orange). Dashed green lines represent H-bonds.

Compared to SR141716A, the imidazolidine-2,4-dione derivatives fit only partially the shape of the binding site. The lipophilic pocket bordered by F2.67, F2.64, H2.65, and F2.61 is left empty, whereas in the case of SR141716A, the piperidine ring is favorably stabilized within that cavity (Figure 6). This might account for the lower CB_1 cannabinoid receptor affinity of these compounds in comparison with SR141716A.

Conclusion

The results reported herein further confirm the interest of the imidazolidine-2,4-dione ring as central scaffold for cannabinoid receptors ligands. Indeed, albeit the 1,5-diphenylimidazolidine-2,4-dione derivatives showed no affinity, the 1,3,5-triphenylimidazolidine-2,4-dione derivatives and the 1,3,5-triphenyl-2-thioxoimidazolidin-4-one derivatives behaved as selective CB_1 cannabinoid receptor ligands. Further, the [^{35}S]-GTPγS assay demonstrated their inverse agonists properties at the human CB_1

cannabinoid receptor. The most active compounds possess a chlorine or bromine substituent in the para position of the N_1 and N_3 phenyl rings, while additional substitution on the C_5 phenyl ring resulted in a decreased affinity. Finally, the compounds 1,3-bis(4-bromophenyl)-5-phenylimidazolidine-2,4-dione (**25**) and 1,3-bis(4-chlorophenyl)-5-phenylimidazolidine-2,4-dione (**23**) are the imidazolidine-2,4-dione derivatives possessing the highest affinity for the human CB_1 cannabinoid receptor reported to date.

Experimental Section

General Procedures. All reagents were purchased from commercial sources (Sigma-Aldrich or Acros) and were used without further purification. Solvents were of analytical grade. [^{3}H]-SR141716A (52 Ci/mol) was acquired from Amersham (Roosendaal, The Netherlands), [^{3}H]-CP-55,940 (101 Ci/mol) from NEN Life Science (Zaventem, Belgium), and [^{3}H]-AEA (60 Ci/mmol) from American Radiolabeled Chemical (St Louis, MO). HU-210 was obtained from Tocris (Bristol, UK), while WIN-55,212-2 was purchased from Research Biochemicals International (Boornem, Belgium). SR141716A was a generous gift from Dr. Barth, Sanofi-Synthélabo Research (Montpellier, France).

The microwave oven used was a commercial household microwave oven (frequency 2450 MHz). Melting points (mp) were determined in open capillaries using the Electrothermal 9100 apparatus and are reported uncorrected. Infrared (IR) spectra of compounds dispersed in KBr were recorded using a Perkin-Elmer FT-IR 286 spectrometer, and values are reported as ν in cm^{-1} (see Supporting Information). Nuclear magnetic resonance (^{1}H NMR, ^{13}C NMR) spectra were recorded on a Bruker AM-300 spectrometer at room temperature and analyzed using the WIN NMR software package. Chemical shifts (δ) are reported relative to the tetramethylsilane peak set at 0 ppm. In the case of multiplets, the signals are reported as intervals. Signals are abbreviated as s, singlet; d, doublet; t, triplet; m, multiplet. Coupling constants are expressed in hertz. Mass spectra were recorded on a Finnigan MAT 44S, with an ionization voltage of 70 eV. Elemental analyses were performed on a Carlo Erba EA 1108 analyzer (Carlo Erba, Milano, Italy) and are within ±0.4% of the theoretical values.

A suitable crystal of compound **22** obtained by recrystallization from ethanol was mounted with a quartz fiber on a goniometer head of a CAD4 Nonius diffractometer. After determination of the cell parameter using 25 well-centered reflections, complete diffraction data sets were collected. The structure was solved using direct methods and refined by full matrix least squares on F^2 using the program Shelxl97.[44] All non-hydrogen atoms were treated anisotropically while a riding model was applied for hydrogen atoms. Analytical correction for absorption was introduced.

Crystallographic Data for Compound 22. Colorless plate (0.08 × 0.28 × 0.35 mm); triclinic; $P\bar{1}$: a = 10.079 (2) Å, b = 17.079 (2) Å, c = 21.679 (3) Å, α = 73.4°, β = 81.9°, γ = 86.5°; V = 3622.0 Å^3; Z = 8, μ = 3.24 mm^{-1}; D_x = 1.494 g/cm^3; λ (Cu Kα) = 1.54178 Å; $F(000)$ = 1648; T = 293 K; 9882 unique reflections (R_{int} = 0.009); 937 refined parameters, R_1 = 0.0403 for 9067 $F_o > 4\sigma(F_o)$, R_1 = 0.0445 for all data and wR_2 = 0.1049, GOF = S = 1.03; $\Delta\rho_{min}$ = −1.09 e/ Å^3; $\Delta\rho_{max}$ = 0.85 e/ Å^3.

General Procedure for the Synthesis of the 1,5-Diphenyl Derivatives (8−14). The synthesis of **6** and **7** was previously described.[37] The 1,5-diphenyl derivatives were synthesized following a method adapted from Joshi et al.[34] Phenylglyoxal (**2**, 4.5 mmol) and phenylurea (**5**, X′ = O) or phenylthiourea (**5**, X′ = S) (4.5 mmol) were refluxed for 4 h in 15 mL of glacial acetic acid in the presence of 0.5 mL of hydrochloric acid. After cooling, the mixture was poured into water and the resulting precipitate filtered off. The residue was subsequently crystallized from ethanol.

1-(4-Chlorophenyl)-5-phenylimidazolidine-2,4-dione (8). Yield: 64%. Mp: 213.1−214.0 °C. MS (EI): 286 [M]$^+$. ^{1}H NMR (DMSO-d_6): δ 5.95 (s, 1H), 7.33−7.55 (m, 9H), 11.49 (s, 1H). ^{13}C NMR (DMSO-d_6): δ 64.87 (CH), 122.77, 127.56, 128.53, 129.05, 129.30, and 134.10, (C and $CH_{arom.}$), 155.18 (C═O), 171.69 (C═O).

1-(4-Bromophenyl)-5-phenylimidazolidine-2,4-dione (9). Yield: 60%. Mp: 216.2−216.8 °C. MS (EI): 332 [M + H]$^+$. ^{1}H NMR (DMSO-d_6): δ 5.94 (s, 1H), 7.34−7.46 (m, 9H), 11.50 (s, 1H). ^{13}C NMR (DMSO-d_6): δ 64.74 (CH), 116.56, 123.03, 127.56, 129.05, 129.31, 131.90, 134.10, and 136.36 (C and $CH_{arom.}$), 155.18 (C═O), 171.68 (C═O).

1-(4-Iodophenyl)-5-phenylimidazolidine-2,4-dione (10). Yield: 58%. Mp: 236.3−237.2 °C. MS (EI): 378 [M]$^+$. ^{1}H NMR (DMSO-d_6): δ 5.94 (s, 1H), 7.32−7.64 (m, 9H), 11.53 (s, 1H). ^{13}C NMR (DMSO-d_6): δ 64.67 (CH), 88.67, 123.23, 127.56, 129.05, 129.37, 134.09, 136.87, and 137.78 (C and $CH_{arom.}$), 155.12 (C═O), 171.62 (C═O). Anal. Calcd for $C_{15}H_{11}IN_2O_2$: C, H, N.

1-(4-Methoxyphenyl)-5-phenylimidazolidine-2,4-dione (11). Yield: 64%. Mp: 151.7−152.6 °C. MS (EI): 282 [M]$^+$. ^{1}H NMR (DMSO-d_6): δ 3.70 (s, 3H), 5.92 (s, 1H), 6.87−7.42 (m, 9H), 11.35 (s, 1H). ^{13}C NMR (DMSO-d_6): δ 55.55 (CH_3), 65.45 (CH), 114.36, 123.74, 127.69, 128.85, 129.24, 129.76, 134.55, and 156.61 (C and $CH_{arom.}$), 155.25 (C═O), 172.07 (C═O).

5-(4-Bromophenyl)-1-phenylimidazolidine-2,4-dione (12). Yield: 60%. Mp: 203.1−204.2 °C. MS (EI): 332 [M]$^+$. ^{1}H NMR (DMSO-d_6): δ 6.00 (s, 1H), 7.02−7.56 (m, 9H), 11.50 (s, 1H). ^{13}C NMR (DMSO-d_6): δ 64.29 (CH), 121.29, 122.26, 124.65, 129.18, 129.82, 132.22, 133.90, and 136.81 (C and $CH_{arom.}$), 155.12 (C═O), 171.49 (C═O).

5-(4-Bromophenyl)-1-(4-chlorophenyl)imidazolidine-2,4-dione (13). Yield: 64%. Mp: 205.1−205.9 °C. MS (EI): 366 [M]$^+$. ^{1}H NMR (DMSO-d_6): δ 5.98 (s, 1H), 7.32−7.58 (m, 8H), 11.55 (s, 1H). ^{13}C NMR (DMSO-d_6): δ 64.41 (CH), 122.16, 122.99, 129.31, 130.08, 132.54, 133.77, and 136.04 (C and $CH_{arom.}$), 155.32 (C═O), 171.49 (C═O).

1,5-Bis(4-bromophenyl)imidazolidine-2,4-dione (14). Yield: 62%. Mp: 242.1−243.0 °C. MS (EI): 410 [M]$^+$. ^{1}H NMR (DMSO-d_6): δ 5.97 (s, 1H), 7.31−7.57 (m, 8H), 11.54 (s, 1H). ^{13}C NMR (DMSO-d_6): δ 64.41 (CH), 122.64, 123.29, 130.02, 132.28, 132.54, 133.77, and 136.49 (C and $CH_{arom.}$), 155.32 (C═O), 171.49 (C═O).

Synthesis of 3-Benzoyl-1,5-diphenylimidazolidine-2,4-dione (15). 1,5-Diphenylimidazolidine-2,4-dione (**6**) (1.98 mmol) was dissolved in a mixture of freshly distilled dichloromethane (25 mL) and pyridine (0.2 mL) under nitrogen prior to the addition of benzoyl chloride (1.98 mmol). The resulting mixture was stirred overnight at room temperature and subsequently washed by $NaHCO_3$ 5%, citric acid 5%, and brine. The resulting organic layer was dried over $MgSO_4$ and evaporated to dryness. The resulting solid was crystallized from ethanol. The formation of **15** was confirmed by the disappearance of the NH peak of **6** in ^{1}H NMR (δ = 11.49 ppm) and by the appearance of one additional carbonyl peak in ^{13}C NMR (δ = 166.45 ppm). Yield: 75%. Mp: 183.5−183.9 °C. MS (EI): 356 [M]$^+$. ^{1}H NMR (DMSO-d_6): δ 6.20 (s, 1H), 7.10−8.04 (m, 15H). ^{13}C NMR (DMSO-d_6): δ 64.41 (CH), 122.19, 125.43, 127.76, 128.98, 129.24, 130.54, 131.96, 133.26, 135.07, and 135.78 (C and $CH_{arom.}$), 151.24 (C═O), 166.45 (C═O), 168.58 (C═O).

Synthesis of 3-Hexanoyl-1,5-diphenylimidazolidine-2,4-dione (16). This derivative was synthesized as **15**, using hexanoyl chloride instead of benzoyl chloride. Yield: 73%. Mp: 133.7−134.6 °C. MS (EI): 350 [M]$^+$. ^{1}H NMR (DMSO-d_6): δ 0.87 (s, 3H), 1.29 (m, 4H), 1.60 (m, 2H), 2.96 (t, J = 7.3, 2H), 6.01 (s, 1H), 7.10−7.35 (m, 10H). ^{13}C NMR (DMSO-d_6): δ 14.14 (CH_3), 22.17, 23.46, 30.90, and 38.01 (CH_2), 63.51 (CH), 121.28, 122.77, 125.75, 127.56, 128.14, 129.24, 133.71, and 135.97 (C and $CH_{arom.}$), 151.37 (C═O), 168.58 (C═O), 171.75 (C═O). Anal. Calcd for $C_{21}H_{22}N_2O_3$: C, H, N.

Synthesis of 3-Pentyl-1,5-diphenylimidazolidine-2,4-dione (17) and 3-Heptyl-1,5-diphenylimidazolidine-2,4-dione (18). To a mixture of **6** (1.98 mmol), K_2CO_3 (7.9 mmol), and tetrabutylammonium bromide (0.19 mmol) in DMF (2 mL) was added the chloroalkyl derivative (2.6 mmol) under stirring. The resulting mixture (in a open flask) was placed in a microwave oven and three 1.5-min pulses (100 W) were applied. After cooling, the mixture was poured into water and extracted with $CHCl_3$. The

organic layer was washed with HCl, NaOH, and brine. The resulting organic phase was dried over $MgSO_4$ and evaporated to dryness. The yields obtained (55 and 59%) were higher than those we previously obtained using another alkylating procedure, i.e. DMF, K_2CO_3, 24 h of stirring (yield 35%).[37]

3-Pentyl-1,5-diphenylimidazolidine-2,4-dione (17). Yield: 59%. Mp: 98.1−99.0 °C. MS (EI): 323 $[M]^+$. ^{1}H NMR (DMSO-d_6): δ 0.82−0.87 (m, 3H), 1.27−1.28 (m, 4H), 1.57−1.62 (m, 2H), 3.51 (t, J = 7.4, 2H), 6.02 (s, 1H), 7.04−7.43 (m, 10H). ^{13}C NMR (DMSO-d_6): δ 13.72 (CH_3), 21.54, 26.98, 28.90, and 38.36 (CH_2), 63.15 (CH), 120.85, 124.29, 127.13, 128.62, 128.62, 128.75, 128.88, 133.66 (C and $CH_{arom.}$), 154.31 (C═O), 170.22 (C═O). Anal. Calcd for $C_{20}H_{22}N_2O_2$: C, H, N.

3-Heptyl-1,5-diphenylimidazolidine-2,4-dione (18). Yield: 57%. Mp: 66.5−67.8 °C. MS (EI): 350 $[M]^+$. ^{1}H NMR (DMSO-d_6): δ 0.81−0.83 (m, 3H), 1.23−1.26 (m, 8H), 1.56−1.59 (m, 2H), 3.50 (t, J = 7.3, 2H), 6.01 (s, 1H), 7.06−7.53 (m, 10H). ^{13}C NMR (DMSO-d_6): δ 13.62 (CH_3), 21.71, 25.72, 27.08, 27.86, and 30.84 (CH_2), 62.92 (CH), 120.70, 124.13, 126.98, 128.40, 128.53, 128.73, 133.64, and 136.17 (C and $CH_{arom.}$), 155.15 (C═O), 170.07 (C═O). Anal. Calcd for $C_{22}H_{26}N_2O_2$: C, H, N.

General Procedure for the Synthesis of 1,3,5-Triphenylimidazolidine-2,4-dione Derivatives (20−29). The phenylglyoxal (**2**) (5 mmol) and 1,3-diphenylurea (**19**, X′ = O) (5 mmol) were refluxed with stirring in concentrated acetic acid (20 mL) and concentrated hydrochloric acid (0.5 mL). After 6 h, the solution was allowed to cool and then poured into water. The resulting precipitate was filtered, dried, and recrystallized from ethanol.

1,3,5-Triphenylimidazolidine-2,4-dione (20). Yield: 60%. Mp: 119.9−120.9 °C. MS DEI: 328 $[M]^+$. ^{1}H NMR (DMSO-d_6): δ 6.71 (s, 1H), 7.31−7.61 (m, 15H). ^{13}C NMR (DMSO-d_6): δ 63.64 (CH), 121.54, 124.84, 127.30, 127.75, 128.05, 128.46, 128.92, 129.11, 129.54, 131.96, 133.97, and 136.42 (C and $CH_{arom.}$), 153.51 (C═O), 169.62 (C═O).

5-(4-Chlorophenyl)-1,3-diphenylimidazolidine-2,4-dione (21). Yield: 51%. Mp: 158.1−158.7 °C. MS DEI: 362 $[M]^+$. ^{1}H NMR (DMSO-d_6): δ 6.21 (s, 1H), 7.11−7.60 (m, 14H). ^{13}C NMR (DMSO-d_6): δ 63.19 (CH), 121.87, 125.17, 125.49, 127.49, 128.73, 129.24, 129.37, 129.95, 132.16, 133.19, 133.97, and 136.55 (C and $CH_{arom.}$), 153.70 (C═O), 169.52 (C═O). Anal. Calcd for $C_{21}H_{15}ClN_2O_2$: C, H, N.

5-(4-Bromophenyl)-1,3-diphenylimidazolidine-2,4-dione (22). Yield: 53%. Mp: 174.4−175.1 °C. MS DEI: 408 $[M + H]^+$. ^{1}H NMR (DMSO-d_6): δ 6.20 (s, 1H), 7.09−7.60 (m, 14H). ^{13}C NMR (DMSO-d_6): δ 62.99 (CH), 121.55, 122.32, 124.91, 127.30, 128.53, 128.98, 130.02, 131.64, 131.90, 132.03, 133.32, and 136.29 (C and $CH_{arom.}$), 153.44 (C═O), 169.23 (C═O). Anal. Calcd for $C_{21}H_{15}BrN_2O_2$: C, H, N.

1,3-Bis(4-chlorophenyl)-5-phenylimidazolidine-2,4-dione (23). Yield: 48%. Mp: 190.8−191.8 °C. MS DEI: 396 $[M]^+$. ^{1}H NMR (DMSO-d_6): δ 6.13 (s, 1H), 7.34−7.58 (m, 13H). ^{13}C NMR (DMSO-d_6): δ 63.83 (CH), 123.36, 126.59, 126.78, 128.08, 129.05, 129.37, 130.99, 133.26, 133.71, 134.16, 135.52, and 135.84 (C and $CH_{arom.}$), 153.44 (C═O), 169.49 (C═O). Anal. Calcd for $C_{21}H_{14}Cl_2N_2O_2$: C, H, N.

1,3-Bis(3-chlorophenyl)-5-phenylimidazolidine-2,4-dione (24). Yield: 48%. Mp: 117.5−118.6 °C. MS DEI: 396 $[M]^+$. ^{1}H NMR (DMSO-d_6): δ 6.19 (s, 1H), 7.16−7.79 (m, 13H). ^{13}C NMR (DMSO-d_6): δ 63.76 (CH), 120.06, 121.54, 124.97, 126.27, 127.43, 128.21, 128.79, 129.37, 130.86, 133.38, 133.64, and 137.98 (C and $CH_{arom.}$), 153.38 (C═O), 169.36 (C═O). Anal. Calcd for $C_{21}H_{14}Cl_2N_2O_2$: C, H, N.

1,3-Bis(4-bromophenyl)-5-phenylimidazolidine-2,4-dione (25). Yield: 54%. Mp: 211.4−212.5 °C. MS DEI: 486 $[M]^+$. ^{1}H NMR (DMSO-d_6): δ 6.14 (s, 1H), 7.36−7.76 (m, 13H). ^{13}C NMR (DMSO-d_6): δ 63.83 (CH), 117.40, 121.80, 123.80, 126.91, 128.21, 129.44, 129.63, 131.44, 132.16, 132.41, 133.71, and 136.08 (C and $CH_{arom.}$), 153.44 (C═O), 169.55 (C═O). Anal. Calcd for $C_{21}H_{14}Br_2N_2O_2$: C, H, N.

1,3-Bis(4-methoxyphenyl)-5-phenylimidazolidine-2,4-dione (26). Yield: 56%. Mp: 140.4−141.3 °C. MS DEI: 388 $[M]^+$. ^{1}H NMR (DMSO-d_6): δ 3.68 (s, 3H), 3.80 (s, 3H), 6.05 (s, 1H), 6.87−7.46 (m, 13H). ^{13}C NMR (DMSO-d_6): δ 55.31 (2×OMe), 63.92 (CH), 114.07, 123.71, 124.41, 127.65, 128.36, 128.62, 128.81, 129.01, 133.86, and 133.95 (C and $CH_{arom.}$), 153.66 (C═O), 156.44 and 158.90 ($C_{arom.}$), 169.77 (C═O). Anal. Calcd for $C_{23}H_{20}N_2O_4$: C, H, N.

1,3,5-Tris(4-chlorophenyl)imidazolidine-2,4-dione (27). Yield: 50%. Mp: 187.1−187.9 °C. MS DEI: 430 $[M]^+$. ^{1}H NMR (DMSO-d_6): δ 6.18 (s, 1H), 7.40−7.61 (m, 12H). ^{13}C NMR (DMSO-d_6): δ 62.63 (CH), 122.86, 122.98, 126.23, 128.44, 128.65, 128.88, 129.66, 130.43, 132.18, 132.82, 133.67, and 134.90 (C and $CH_{arom.}$), 152.95 (C═O), 168.73 (C═O). Anal. Calcd for $C_{21}H_{13}Cl_3N_2O_2$: C, H, N.

1,3-Bis(3-chlorophenyl)-5-(4-chlorophenyl)imidazolidine-2,4-dione (28). Yield: 48%. Mp: 80.8−81.4 °C. MS DEI: 430 $[M]^+$. ^{1}H NMR (DMSO-d_6): δ 6.21 (s, 1H), 7.18−7.76 (m, 12H). ^{13}C NMR (DMSO-d_6): δ 62.99 (CH), 120.06, 121.54, 125.04, 126.27, 127.43, 128.85, 129.37, 130.22, 130.92, 132.61, 133.32, 133.64, 134.16, and 137.85 (C and $CH_{arom.}$), 153.31 (C═O), 169.10 (C═O). Anal. Calcd for $C_{21}H_{13}Cl_3N_2O_2$: C, H, N.

5-(4-Bromophenyl)-1,3-bis(4-chlorophenyl)imidazolidine-2,4-dione (29). Yield: 46%. Mp: 197.6−198.5 °C. MS DEI: 476 $[M]^+$. ^{1}H NMR (DMSO-d_6): δ 6.18 (s, 1H), 7.39−7.62 (m, 12H). ^{13}C NMR (DMSO-d_6): δ 63.25 (CH), 122.84, 123.36, 126.72, 129.11, 129.31, 130.47, 130.99, 132.03, 132.35, 133.13, 133.38, and 135.45 (C and $CH_{arom.}$), 153.44 (C═O), 169.16 (C═O). Anal. Calcd for $C_{21}H_{13}BrCl_2N_2O_2$: C, H, N.

General Procedure for the Synthesis of 1,3,5-Triphenyl-2-thioxoimidazolidin-4-one Derivatives (30−38). These compounds were synthesized similarly to the 1,3,5-triphenylimidazolidine-2,4-diones using 1,3-diphenylthiourea (**19**, X′ = S) instead of 1,3-diphenylurea (**19**, X′ = O).

1,3,5-Triphenyl-2-thioxoimidazolidin-4-one (30). Yield: 59%. Mp: 169.1−170.2 °C. MS DEI: 344 $[M]^+$. ^{1}H NMR (DMSO-d_6): δ 6.28 (s, 1H), 7.22−7.60 (m, 15H). ^{13}C NMR (DMSO-d_6): δ 68.49 (CH), 127.04, 127.62, 128.27, 129.11, 129.24, 133.25, 133.96, and 137.33 (C and $CH_{arom.}$), 171.36 (C═O), 181.78 (C═S). Anal. Calcd for $C_{21}H_{16}N_2OS$: C, H,N.

5-(4-Bromophenyl)-1,3-diphenyl-2-thioxoimidazolidin-4-one (31). Yield: 57%. Mp: 193.3−193.7 °C. MS DEI: 423 $[M]^+$. ^{1}H NMR (DMSO-d_6): δ 6.28 (s, 1H), 7.23−7.68 (m, 14H). ^{13}C NMR (DMSO-d_6): δ 68.26 (CH), 126.81, 127.39, 128.04, 128.62, 128.88, 129.01, 133.02, 133.73, 134.10, 134.64, and 137.10 (C and $CH_{arom.}$), 171.06 (C═O), 181.55 (C═S). Anal. Calcd for $C_{21}H_{15}BrN_2OS$: C, H, N.

1,3-Bis(4-chlorophenyl)-5-phenyl-2-thioxoimidazolidin-4-one (32). Yield: 58%. Mp: 214.9−215.3 °C. MS DEI: 413 $[M]^+$. ^{1}H NMR (DMSO-d_6): δ 6.24 (s, 1H), 7.35−7.63 (m, 13H). ^{13}C NMR (DMSO-d_6): δ 68.36 (CH), 128.41, 128.72, 128.98, 129.17, 129.31, 129.44, 131.05, 132.02, 132.67, 132.86, 133.83, and 136.10 (C and $CH_{arom.}$), 171.04 (C═O), 181.52 (C═S). Anal. Calcd for $C_{21}H_{14}Cl_2N_2OS$: C, H, N.

1,3-Bis(4,3-dichlorophenyl)-5-phenyl-2-thioxoimidazolidin-4-one (33). Yield: 52%. Mp: 172.6−173.7 °C. MS DEI: 482 $[M]^+$. ^{1}H NMR (DMSO-d_6): δ 6.29 (s, 1H), 7.37−7.97 (m, 11H). ^{13}C NMR (DMSO-d_6): δ 68.43 (CH), 127.49, 128.85, 129.11, 129.57, 129.82, 129.96, 131.12, 131.38, 131.57, 132.80, 133.40, 133.84, and 137.27 (C and $CH_{arom.}$), 170.85 (C═O), 181.65 (C═S). Anal. Calcd for $C_{21}H_{12}Cl_4N_2OS$: C, H, N.

1,3-Bis(4-bromophenyl)-5-phenyl-2-thioxoimidazolidin-4-one (34). Yield: 54%. Mp: 233.4−234.5 °C. MS DEI: 502 $[M]^+$. ^{1}H NMR (DMSO-d_6): δ 6.23 (s, 1H), 7.35−7.77 (m, 13H). ^{13}C NMR (DMSO-d_6): δ 68.30 (CH), 120.51, 122.45, 128.40, 128.98, 129.31, 129.44, 131.31, 131.90, 132.16, 132.80, 133.13, and 136.49 (C and $CH_{arom.}$), 170.91 (C═O), 181.39 (C═S). Anal. Calcd for $C_{21}H_{14}Br_2N_2OS$: C, H, N.

1,3-Bis(3-iodophenyl)-5-phenyl-2-thioxoimidazolidin-4-one (35). Yield: 49%. Mp: 182.3−182.9 °C. MS DEI: 596 $[M]^+$. ^{1}H NMR (DMSO-d_6): δ 6.21 (s, 1H), 7.14−8.01 (m, 13H). ^{13}C NMR (DMSO-d_6): δ 68.42 (CH), 94.04, 126.52, 128.53, 128.79, 129.24, 129.44, 130.80, 130.99, 132.87, 135.00, 135.52, 136.43, 137.52,

137.91, and 138.43 (C and $CH_{arom.}$), 170.98 (C=O), 181.95 (C=S). Anal. Calcd for $C_{21}H_{14}I_2N_2OS$: C, H, N.

1,3-Bis(4-methylphenyl)-5-phenyl-2-thioxoimidazolidin-4-one (36). Yield: 63%. Mp: 191.2−192.0 °C. MS DEI: 372 $[M]^+$. ^{1}H NMR (DMSO-d_6): δ 2.24 (s, 3H), 2.37 (s, 3H), 6.19 (s, 1H), 7.14−7.44 (m, 13H). ^{13}C NMR (DMSO-d_6): δ 20.68 (Me), 20.69 (Me), 68.43 (CH), 126.07, 126.78, 128.21, 128.85, 129.24, 129.37, 129.57, 131.38, 133.32, 134.80, 137.07, and 138.63 (C and $CH_{arom.}$), 171.43 (C=O), 181.91 (C=S). Anal. Calcd for $C_{23}H_{20}N_2OS$: C, H, N.

1,3-Bis(4-methoxyphenyl)-5-phenyl-2-thioxoimidazolidin-4-one (37). Yield: 58%. Mp: 188.0−188.9 °C. MS DEI: 404 $[M]^+$. ^{1}H NMR (DMSO-d_6): δ 3.71 (s, 3H), 3.81 (s,3H), 6.13 (s, 1H), 6.85−7.44 (m, 13H). ^{13}C NMR (DMSO-d_6): δ 55.12 (OMe), 55.32 (OMe), 68.45 (CH), 113.80, 114.00, 126.29, 128.04, 128.43, 128.95, 129.53, 129.98, 130.24, 133.15, 158.06, and 159.29 (C and $CH_{arom.}$), 171.39 (C=O), 182.13 (C=S). Anal. Calcd for $C_{23}H_{20}N_2O_3S$: C, H, N.

1,3-Bis(4-hydroxyphenyl)-5-phenyl-2-thioxoimidazolidin-4-one (38). To a solution of **37** in freshly distilled CH_2Cl_2 (1 mM) kept in an ice bath was added boron tribromide (1.2 mM) under stirring. The solution was then allowed to reach room temperature and stirred overnight. The resulting solution was evaporated to dryness under reduced pressure and the resulting solid washed with water. After filtration, the compound was crystallized from ethanol. Yield: 75%. Mp: 199.2−200.0 °C. MS DEI: 376 $[M]^+$. ^{1}H NMR (DMSO-d_6): δ 6.05 (s, 1H), 6.66−7.44 (m, 13H), 9.61 (s, 1H), 9.87 (s, 1H). ^{13}C NMR (DMSO-d_6): δ 68.68 (CH), 115.34, 115.53, 125.10, 128.21, 128.40, 128.66, 129.17, 130.15, 133.54, 156.67, and 157.84 (C and $CH_{arom.}$), 171.75 (C=O), 182.49 (C=S). Anal. Calcd for $C_{21}H_{16}N_2O_3S$: C, H, N.

1,3-Dicyclohexyl-5-phenylimidazolidine-2,4-dione (40) was synthesized as derivatives **20**−**29**, with 1,3-dicyclohexylurea (**39**) instead of 1,3-diphenylurea, and recrystallized from hexane−acetone. Yield: 46%. Mp: 99.2−99.8 °C. MS DEI: 340 $[M]^+$. ^{1}H NMR (DMSO-d_6): δ 0.68−2.09 (m, 20H), 3.49−3.58 (m, 1H), 3.73−3.81 (m, 1H), 5.17 (s, 1H), 7.28−7.36 (m, 5H). ^{13}C NMR (DMSO-d_6): δ 24.95, 25.34, 35.47, 29.22, 29.93, and 31.41 (CH_2), 50.89, 53.22, and 61.63 (CH), 127.62, 128.73, 128.99, and 136.43 (C and $CH_{arom.}$), 153.44 (C=O), 169.16 (C=O). Anal. Calcd for $C_{21}H_{28}N_2O_2$: C, H, N.

Cell Culture and Preparation of *h*CB_1- or *h*CB_2-Transfected CHO Cell Membranes. Chinese hamster ovarian (CHO) cells stably transfected with the cDNA sequences encoding either the human CB_1 or the human CB_2 cannabinoid receptors were kindly donated by Dr. M. Detheux and Dr. P. Nokin, respectively (Euroscreen s.a., Gosselies, Belgium). Cells were grown in Ham's F12 nutrient mixture supplemented with 10% FBS, 2.5 μL/mL fungizone, 100 U/mL penicillin, 100 μg/mL streptomycin, and 400 μg/mL G418. Once at confluence, cells were trypsinized and collected by centrifugation at 100*g* for 10 min. The following steps were performed on ice. Pellet was lysed in ice-cold 50 mM Tris-HCl, pH 7.4, and the homogenate was centrifuged at 15 000*g* for 10 min. The resulting pellet (membranes) was washed twice with the same solution under identical conditions. Protein content was determined as described by Bradford using Coomasie Blue (Bio-Rad, Belgium) with bovine serum albumin as standard.

Preparation of Rat Cerebellum Membranes. Male Wistar rats (250−300 g) were purchased from IFFA-CREDO (Les Oncins, France). All experiments on animals were approved by the institutional ethics committee and the housing conditions were as specified by the Belgian Law of November 14, 1993, on the protection of laboratory animals (agreement no. LA 1230315). Cerebella were carefully dissected on ice. All the manipulations were performed at 0−4°C. Rat cerebellum membranes were prepared in 50 mM Tris-HCl pH 7.4, with a Potter-Elvejhem and a Dounce tissue grinder, and the suspension was centrifuged at 400*g* for 10 min. The supernatant was collected and centrifuged at 39 000*g* for 10 min. The resulting pellet was resuspended in 50 mM Tris-HCl pH 7.4, homogenized, and centrifuged again at 39 000 *g* for 10 min. The pellet was washed twice more under the same conditions. Protein concentration was measured as described for the CHO membranes.

Competition Binding Assay. The assay was performed using CHO cells membranes (or rat cerebellum homogenate) as previously described.[31] Briefly, the competitive binding experiments were performed using [^{3}H]-SR141716A (1 nM) or [^{3}H]-CP-55,940 (1 nM) as radioligands for the *h*CB_1 and the *h*CB_2 cannabinoid receptors, respectively, at 30 °C in plastic tubes, and 40 μg of membranes per tube resuspended in 0.5 mL (final volume) binding buffer (50 mM Tris-HCl, 3 mM $MgCl_2$, 1 mM EDTA, 0.5% bovine serum albumin, pH 7.4). The test compounds were present at varying concentrations, and the nonspecific binding was determined in the presence of 10 μM HU-210. After 1 h the incubation was stopped, and solutions were rapidly filtered through 0.5% PEI pretreated GF/B glass fiber filters (Whatman, Maidstone, UK) on a M-48T Brandell cell harvester and washed twice with 5 mL of ice-cold binding buffer without serum albumin. The radioactivity on the filters was measured in a Pharmacia Wallac 1410 β-counter using 10 mL of Aqualuma (PerkinElmer, Schaesberg, The Netherlands), after 10 s shaking and 3 h resting. Assays were performed at least in triplicate. Final DMSO concentrations in the assay were less than 0.1%.

Under these conditions, using [^{3}H]-SR141716A, the B_{max} value was 57 pmol/mg of protein and the K_d value was 1.13 ± 0.13 nM for the *h*CB_1 cannabinoid receptor.

The competition binding assays performed on the rat cerebellum were performed in the presence of 100 μg of protein per tube. Under these conditions, using [^{3}H]-SR141716A, the B_{max} value was 3.30 pmol/mg of protein and the K_d value was 3.11 ± 0.15 nM for the *h*CB_1 cannabinoid receptor.

[^{35}S]-GTPγS Assay. [^{35}S]-GTPγS (1173 Ci/mmol) was obtained from Amersham (Roosendaal, The Netherlands). The binding experiments were performed at 30 °C in plastic tubes containing 40 μg of protein (CHO cells homogenate or rat cerebellum homogenate) in 0.5 mL (final volume) of binding buffer (50 mM Tris-HCl, 3 mM $MgCl_2$, 1 mM EDTA, 100 mM NaCl, 0.1% bovine serum albumin, pH 7.4) supplemented with 20 μM GDP and varying concentrations of the test compounds. The assay was initiated by the addition of [^{35}S]-GTPγS (0.05 nM, final concentration). The tubes were incubated for 1 h. The incubations were terminated by the addition of 5 mL of ice-cold washing buffer (50 mM Tris-HCl, 3 mM $MgCl_2$, 1 mM EDTA, 100 mM NaCl). The suspension was immediately filtered through GF/B filters using a 48-well Brandell cell harvester and washed twice with the same ice-cold buffer. The radioactivity on the filters was counted as mentioned above. Nonspecific binding was measured in the presence of 100 μM Gpp(NH)p. Assays were performed in triplicate.

Brain Membrane Preparation for FAAH Assay. Adult rat brains were homogenized at 4°C in homogenization buffer (20mM HEPES, 1 mM $MgCl_2$, pH 7.0) using a tissue grinder and subsequently centrifuged for 20 min at 36 000 *g*. The pellet was resuspended in homogenization buffer and centrifuged again for 20 min at 36 000 *g*. The latter operation was performed twice. The resulting pellet was stored in a conservation buffer (50 mM Tris.HCl, 1 mM EDTA, 3 mM $MgCl_2$, pH 7.6). Membranes aliquots were stored at −80 °C until use. The protein content was determined as for CHO cells membranes.

Fatty Acid Amide Hydrolase Inhibition Assay. Compounds were assayed as described by Jonsson et al.[45] Membranes, test compounds or DMSO (10 μL), [^{3}H]-AEA (50.000 dpm; 2 μM final concentration), and assay buffer (10 mM Tris-HCl, 1 mM EDTA, 0.1% (w/v) BSA, pH 7.6) were incubated at 37 °C for 10 min. Reactions were stopped by rapidly placing the tubes in ice and adding 400 μL of chloroform/methanol (1:1 v/v) followed by vigorous mixing. Phases were separated by centrifugation at 850*g* and aliquots (200 μL) of the upper methanol/buffer phase were counted for radioactivity by liquid scintillation counting (Pharmacia Wallac 1410 β-counter). Blanks contained buffer instead of the homogenate preparations.

Molecular Modeling. All computational experiments were conducted on a Silicon Graphics Octane2 workstation, running under the IRIX 6.5 operating system. Molecular modeling studies were carried out using the InsightII software[46] (version 2000). The input structure of both enantiomers of **25** was based on the crystallographic conformation of **22**. The coordinates of the CB_1 cannabinoid receptor model were kindly provided by Dr. O. M. Salo. The original model[40] was modified to the inactive R-state, and several residues had to be rotated in order to enable the accurate docking of SR141716A and of our derivatives.

Docking of both enantiomers of **25** was carried out using the genetic algorithm GOLD (version 3.0).[42] It performs docking of flexible ligands into proteins with partial flexibility in the neighborhood of the active site. The torsion angles of Ser, Thr, and Tyr hydroxyl groups as well as Lys NH_3^+ moieties are optimized during the run so that hydrogen-bond formation is favored. Defaults settings were used for the genetic algorithm parameters. To take protein flexibility into account, the complexes were then refined with Discover3 (CVFF force field, dielectric constant = r).[43] The energetic minimization process consists of two sequential steps: the Steepest Descent algorithm, reaching a final convergence of 10.0 kcal mol^{-1} $Å^{-1}$, followed by the Conjugate Gradient algorithm to reach a final convergence of 0.01 kcal mol^{-1} $Å^{-1}$. First, all the protein's atoms were held fixed, and only the orientation of the ligand was optimized. Then, the α-C atoms of the binding site's residues (sphere of 18.0 Å around the nitrogen atom of K3.28) were relaxed. A tethering restraint was applied on these atoms, to keep them from moving too far from their original positions. This restraint had a quadratic form with a constant force of 20 kcal $Å^{-2}$ and was progressively decreased (scale factors of 0.5 and 0.25).

Data Analysis. IC_{50} values were determined by nonlinear regression analysis performed using the GraphPad prism program (GraphPad Software, San Diego, CA). The K_i values were calculated following the Cheng−Prusoff equation: $K_i = IC_{50}/(1 + L/K_d)$. The statistical significance of [^{35}S]-GTPγS results was assessed using one-way ANOVA followed by a Dunett post-test.

Acknowledgment. The authors wish to thank François Abbeloos for technical assistance. T.P., P.D.P., and P.D.M. are exchange pregraduate students from Università degli Studi di Salerno (Italy). One of us (G.G.M.) is very indebted to "Fonds pour la formation à la Recherche dans l'Industrie et l'Agriculture (FRIA)" for the award of a research fellowship. This work was partially funded by a FRSM grant (Belgian National Fund for Scientific Research) and a FSR grant (Université catholique de Louvain).

Supporting Information Available: Procedures for the synthesis of substituted phenylglyoxal and substituted urea and thiourea derivatives, characteristic IR peaks, elemental analysis results of original compounds, and X-ray structure data for **22**. This material is available free of charge via the Internet at http://pubs.acs.org.

References

(1) Matsuda, L. A.; Lolait, S. J.; Brownstein, M. J.; Young, A. C.; Bonner, T. I. Structure of a Cannabinoid Receptor and Functionnal Expression of the Cloned cDNA. *Nature* **1990**, *346*, 561−564.
(2) Munro, S.; Thomas, K. L.; Abu-Shaar, M. Molecular Characterization of a Peripheral Receptor for Cannabinoids. *Nature* **1993**, *365*, 61−65.
(3) Devane, W. A.; Hanus, L.; Breuer, A.; Pertwee, R. G.; Stevenson, L. A.; Griffin, G.; Gibson, D.; Mandelbaum, A.; Etinger, A.; Mechoulam, R. Isolation and Structure of a Brain Constituent That Binds to the Cannabinoid Receptor. *Science* **1992**, *258*, 1946−1949.
(4) Mechoulam, R.; Ben-Shabat, S.; Hanus, L.; Ligumsky, M.; Kaminski, N. E.; Schatz, A. R.; Gopher, A.; Almong, S.; Martin, B. R.; Compton, D. R.; Pertwee, R. G.; Griffin, G.; Bayewitch, M.; Barg, J.; Vogel, Z. Identification of an Endogenous 2-Monoglyceride, Present in Canine Gut, that Binds to Cannabinoid Receptors. *Biochem. Pharmacol*. **1995**, *50*, 83−90.
(5) Sugiura, T.; Kondo, S.; Sukagawa, A.; Nakane, S.; Shinoda, A.; Itoh, K.; Yamashita, A.; Waku, K. 2-Arachidonoylglycerol: a Possible Endogenous Cannabinoid Receptor Ligand in Brain. *Biochem. Biophys. Res. Commun.* **1995**, *215*, 89−97.
(6) Cravatt, B. F.; Giang, D. K.; Mayfield, S. P.; Boger, D. L.; Lerner, R. A.; Gilula, N. B. Molecular Characterization of an Enzyme That Degrades Neuromodulatory Fatty-Acid Amides. *Nature* **1996**, *384*, 83−87.
(7) Karlsson, M.; Contreras, J. A.; Hellman, U.; Tornqvist, H.; Holm, C. cDNA Cloning, Tissue Distribution, and Identification of the Catalytic Triad of Monoglyceride Lipase. Evolutionary Relationship To Esterases, Lysophospholipases, And Haloperoxidases. *J. Biol. Chem.* **1997**, *272*, 27218−27223.
(8) Tsuboi, K.; Sun, Y. X.; Okamoto, Y.; Araki, N.; Tonai, T.; Ueda, N. Molecular Characterization of *N*-Acylethanolamine-Hydrolyzing Acid Amidase, a Novel Member of the Choloylglycine Hydrolase Family with Structural and Functional Similarity to Acid Ceramidase. *J. Biol. Chem.* **2005**, *280*, 11082−11092.
(9) Lambert, D. M.; Fowler, C. J. The Endocannabinoid System: Drug Targets, Lead Compounds and Potential Therapeutic Applications. *J. Med. Chem*. **2005**, *48*, 5059−5087.
(10) Notcutt, W.; Price, M.; Miller, R.; Newport, S.; Phillips, C.; Simmons. S.; Sansom, C. Initial Experiences with Medicinal Extracts of Cannabis for Chronic Pain: Results from 34 'N of 1' studies. *Anaesthesia* **2004**, *59*, 440−52.
(11) Muller-Vahl, K. R.; Schneider, U.; Prevedel, H.; Theloe, K.; Kolbe, H.; Daldrup, T.; Emrich, H. M. Delta 9-Tetrahydrocannabinol (THC) Is Effective in the Treatment of Tics in Tourette Syndrome: A 6-Week Randomized Trial. *J. Clin. Psychiatry* **2003**, *64*, 459−465.
(12) Zajicek, J.; Fox, P.; Sanders, H.; Wright, D.; Vickery, J.; Nunn, A.; Thompson, A. Cannabinoids for Treatment of Spasticity and Other Symptoms Related to Multiple Sclerosis (CAMS Study): Multicentre Randomised Placebo-Controlled Trial. *Lancet* **2003**, *362*, 1517−1526.
(13) Lange, J. H. M.; Kruse, C. G. Recent Advances in CB_1 Cannabinoid Receptor Antagonists. *Curr. Opin. Drug Discov. Devel*. **2004**, *7*, 498−506.
(14) Lange, J. H. M.; Kruse, C. G. Medicinal Chemistry Strategies to CB_1 Cannabinoid Receptor Antagonists. *Drug Discovery Today* **2005**, *10*, 693−702.
(15) Smith, R. A.; Fathi, Z. Recent Advances in the Research and Development of CB_1 Antagonists. *Idrugs* **2005**, *8*, 53−66.
(16) Rinaldi-Carmona, M.; Barth, F.; Heaulme, M.; Shire, D.; Calandra, B.; Congy, C.; Martinez, S.; Maruani, J.; Neliat, G.; Caput, D. SR141716A, a Potent and Selective Antagonist of the Brain Cannabinoid Receptor. *FEBS Lett.* **1994**, *350*, 240−244.
(17) Van Gaal, L. F.; Rissanen, A. M.; Scheen, A. J.; Ziegler, O.; Rössner, S.; for the RIO−Europe Study Group. Effects of the Cannabinoid-1 Receptor Blocker Rimonabant on Weight Reduction and Cardiovascular Risk Factors in Overweight Patients: 1-Year Experience from the RIO−Europe Study. *Lancet* **2005**, *365*, 1389−1397.
(18) Cleland, J. G. F.; Ghosh, J.; Freemantle, N.; Kaye, G. C.; Nasir, M.; Clark, A. L.; Coletta, A. P. Clinical Trials Update and Cumulative Meta-Analyses from the American College of Cardiology: WATCH, SCD-HeFT, DINAMIT, CASINO, INSPIRE, STRATUS−US, RIO−Lipids and Cardiac Resynchronisation Therapy in Heart Failure. *Eur. J. Heart Fail.* **2005**, *6*, 501−508.
(19) Le Foll, B.; Goldberg, S. R. Cannabinoid CB_1 Receptor Antagonists as Promising New Medications for Drug Dependence. *J. Pharm. Exp. Ther*. **2005**, *312*, 875−883.
(20) Muthian, S.; Rademacher, D. J.; Roelke, C. T.; Gross, G. J.; Hillard, C. J. Anandamide Content is Increased and CB_1 Cannabinoid Receptor Blockade Is Protective During Transient, Focal Cerebral Ischemia. *Neuroscience* **2004**, *129*, 743−750.
(21) Muccioli, G. G.; Lambert, D. M. Current Knowledge on the Antagonists and Inverse Agonists of Cannabinoid Receptors. *Curr. Med. Chem.* **2005**, *12*, 1361−1394.
(22) Rinaldi-Carmona, M.; Barth, F.; Congy, C.; Martinez, S.; Oustric, D.; Perio, A.; Poncelet, M.; Maruani, J.; Arnone, M.; Finance, O.; Soubrie, P.; Le Fur, G. SR147778 [5-(4-Bromophenyl)-1-(2,4-dichlorophenyl)-4-ethyl-*N*-(1-piperidinyl)-1*H*-pyrazole-3-carboxamide], a New Potent and Selective Antagonist of the CB_1 Cannabinoid Receptor: Biochemical and Pharmacological Characterization. *J. Pharmacol. Exp. Ther.* **2004**, *310*, 905−914.
(23) Jagerovic, N.; Hernandez-Folgado, L.; Alkorta, I.; Goya, P.; Navarro, M.; Serrano, A.; Rodriguez de Fonseca, F.; Dannert, M. T.; Alsasua, A.; Suardiaz, M.; Pascual, D.; Martin, M. I. Discovery of 5-(4-Chlorophenyl)-1-(2,4-dichlorophenyl)-3-hexyl-1*H*-1,2,4-triazole, a Novel in Vivo Cannabinoid Antagonist Containing a 1,2,4-Triazole Motif. *J. Med. Chem*. **2004**, *47*, 2939−2942.
(24) Lange, J. H.; van Stuivenberg, H. H.; Coolen, H. K.; Adolfs, T. J.; McCreary, A. C.; Keizer, H. G.; Wals, H. C.; Veerman, W.; Borst, A. J.; de Looff, W.; Verveer, P. C.; Kruse, C. G. Bioisosteric Replacements of the Pyrazole Moiety of Rimonabant: Synthesis, Biological Properties, and Molecular Modeling Investigations of Thiazoles, Triazoles, and Imidazoles as Potent and Selective CB_1 Cannabinoid Receptor Antagonists. *J. Med. Chem.* **2005**, *48*, 1823−1838.

(25) Lange, J. H. M.; Coolen, H. K. A. C.; van Stuivenberg, H. H.; Dijksman, J. A. R.; Herremans, A. H. J.; Ronken, E.; Keizer, H. G.; Tipker, K.; McCreary, A. C.; Veerman, W.; Wals, H. C.; Stork, B.; Verveer, P. C.; den Hartog, A. P.; de Jong, N. M. J.; Adolfs, T. J. P.; Hoogendoorn, J.; Kruse, C. G. Synthesis, Biological Properties, and Molecular Modeling Investigations of Novel 3,4-Diarylpyrazolines as Potent and Selective CB_1 Cannabinoid Receptor Antagonists. *J. Med. Chem.* **2004**, *47*, 627−643.

(26) Plummer, C. W.; Finke, P. E.; Mills, S. G.; Wang, J.; Tong, X.; Doss, G. A.; Fong, T. M.; Lao, J. Z.; Schaeffer, M. T.; Chen, J.; Shen, C. P.; Stribling, D. S.; Shearman, L. P.; Strack, A. M.; Van der Ploeg, L. H. Synthesis and Activity of 4,5-Diarylimidazoles as Human CB_1 Receptor Inverse Agonists. *Bioorg. Med. Chem. Lett*. **2005**, *15*, 1441−1446.

(27) Meurer, L. C.; Finke, P. E.; Mills, S. G.; Walsh, T. F.; Toupence, R. B.; Goulet, M. T.; Wang, J.; Tong, X.; Fong, T. M.; Lao, J.; Schaeffer, M. T.; Chen, J.; Shen, C. P.; Sloan Stribling, D.; Shearman, L. P.; Strack, A. M.; Van der Ploeg, L. H. Synthesis and SAR of 5,6-Diarylpyridines as Human CB_1 Inverse Agonists. *Bioorg. Med. Chem. Lett.* **2005**, *15*, 645−651.

(28) Kanyonyo, M.; Govaerts, S. J.; Hermans, E.; Poupaert, J. H.; Lambert, D. M. 3-Alkyl-(5,5′-diphenyl)imidazolidinediones as New Cannabinoid Receptor Ligands. *Bioorg. Med. Chem. Lett.* **1999**, *9*, 2233−2236.

(29) Muccioli, G. G.; Poupaert, J. H.; Wouters, J.; Norberg, B.; Poppitz, W.; Scriba, G. K. E.; Lambert, D. M. A Rapid and Efficient Microwave-Assisted Synthesis of Hydantoins and Thiohydantoins. *Tetrahedron* **2003**, *59*, 1301−1307.

(30) Ooms, F.; Wouters, J.; Oscari, O.; Happaerts, T.; Bouchard, G.; Carrupt, P.-A.; Testa, B.; Lambert, D. M. Explorations of the Pharmacophore of 3-Alkyl-5-arylimidazolidinediones as New CB_1 Cannabinoid Receptor Ligands and Potential Antagonists: Synthesis, Lipophilicity, Affinity, and Molecular Modeling. *J. Med. Chem.* **2002**, *45*, 1748−1756.

(31) Muccioli, G. G.; Martin, D.; Scriba, G. K. E.; Poppitz, W.; Poupaert, J. H.; Wouters, J.; Lambert, D. M. Substituted 5,5′-Diphenyl-2-thioxoimidazolidin-4-one as CB_1 Cannabinoid Receptor Ligands: Synthesis and Pharmacological Evaluation. *J. Med. Chem.* **2005**, *48*, 2509−2516.

(32) Riley, H. A.; Gray, A. R. In *Organic Synthesis*; Wiley: New York, 1943, Vol. II, pp 509−511.

(33) Kurzer, F. In *Organic Synthesis*; Wiley: New York, 1964, Vol. IV, pp 49−50.

(34) Joshi, K. C.; Pathak, V. N.; Goyal, M. K. Fluorine Containig Bioactive Heterocycles. Part II. Synthesis of Some New Fluorine Containnig Arylglyoxals, Their Hydrates and 1,5-Disubstituted Hydantoins. *J. Heterocycl. Chem.* **1981**, *18*, 1651−1653.

(35) Bogdal, D.; Pielichowski, J.; Boron, A. Remarkable Fast Microwave-Assisted *N*-Alkylation of Phthalimide in Dry Media. *Synlett* **1996**, *9*, 873−874.

(36) Foces-Foces, C.; Jagerovic, N.; Elguero, J. Crystal Structure of 1,3,5-Triphenyl-2-pyrazoline: A Case of Spontaneous Resolution. *Z. Kristallogr.* **2001**, *216*, 240−244.

(37) Muccioli, G. G.; Fazio, N.; Scriba, G. K. E.; Poppitz, W.; Cannata, F.; Poupaert, J. H.; Wouters, J.; Lambert, D. M. Substituted 2-Thioxoimidazolidin-4-ones and Imidazolidin-2,4-diones as Fatty Acid Amide Hydrolase Inhibitors Templates. *J. Med. Chem.* **2005**, ASAP Article; DOI: 10.1021/jm050977k.

(38) Harrison, C.; Traynor, J. R. The [^{35}S]-GTPγS Binding Assay: Approaches and Applications in Pharmacology. *Life Sci.* **2003**, *74*, 489−508.

(39) Govaerts, S. J.; Muccioli; G. G.; Hermans; E.; Lambert, D. M. Characterization of the Pharmacology of Imidazolidinedione Derivatives at Cannabinoid CB_1 and CB_2 Receptors. *Eur. J. Pharmacol*. **2004**, *495*, 43−53.

(40) Salo, O. M.; Lahtela-Kakkonen, M.; Gynther, J.; Jarvinen, T.; Poso, A. Development of a 3D Model for the Human Cannabinoid CB_1 Receptor. *J. Med. Chem.* **2004**, *47*, 3048−3057.

(41) Hurst, D. P.; Lynch, D. L.; Barnett-Norris, J.; Hyatt, S. M.; Seltzman, H. H.; Zhong, M.; Song, Z. H.; Nie, J.; Lewis, D.; Reggio, P. H. *N*-(Piperidin-1-yl)-5-(4-chlorophenyl)-1-(2,4-dichlorophenyl)-4-methyl-1*H*-pyrazole-3-carboxamide (SR141716A) Interaction with Lys 3.28(192) Is Crucial for Its Inverse Agonism at the Cannabinoid CB1 Receptor. *Mol. Pharmacol.* **2002**, *62*, 1274−1287.

(42) Jones, G.; Willett, P.; Glen, R. C.; Leach, A. R.; Taylor, R. Development and Validation of a Genetic Algorithm for Flexible Docking. *J. Mol. Biol.* **1997**, *267*, 727−748.

(43) *Discover3*, 2.98 ed.; Accelrys Inc.: San Diego, CA.

(44) Sheldrick, G. *Shelxl97: Program for the refinement of molecular crystal structures;* University of Göttingen, Germany, 1997.

(45) Jonsson, K. O.; Vandevoorde, S.; Lambert, D. M.; Tiger, G.; Fowler, C. J. Effects of Homologues and Analogues of Palmitoylethanolamide upon the Inactivation of the Endocannabinoid Anandamide. *Br. J. Pharmacol.* **2001**, *133*, 1263−1275.

(46) *InsightII*; Accelrys Inc. San Diego, CA, 2000.

JM050484F